## PAPER D

# ATTENUATION ESTIMATION FROM FULL WAVEFORM SONIC LOGS USING SHORT-TIME FOURIER TRANSFORM

**Youli Quan and Jerry M. Harris**

## ABSTRACT

Full waveform sonic logs record complete wave trains which consist of P-wave, S-wave, guided waves and so on. We use short-time Fourier transform to analyze these waves and find their centroid frequencies. The change in the centroid frequencies acts as the attenuation indication of a seismic wave in absorptive media. A profile of centroid frequencies provides a new representation of a full waveform sonic log, from which we can qualitatively correlate wave attenuation and velocity, and compare the attenuation of different waves. The way to quantitatively determine the P-wave attenuation is also discussed. Tests on field data are presented.

## INTRODUCTION

Methods of amplitude decay and spectral ratio were used to estimate attenuation from full waveform sonic logs (Cheng et al, 1982; Engelhard et at, 1984). Effects are still being made to develop more reliable methods for routine log interpretations. We here introduce frequency shift method (Dines & Kak, 1979; Quan & Harris, 1993; Fink et al, 1983) to estimate attenuation from full waveform sonic logs. Seismic wave attenuation usually increases with frequency. The high frequency components of the seismic signal are more attenuated than the low frequency components, which results in a frequency down shift in the spectrum of an incident wave during propagation. The frequency shift method uses this down shifting as the information of attenuation.

Full waveform sonic logs are complete seismograms recorded using an array sonic tool inside a fluid-filled borehole. The array sonic tool includes an array of receivers and a source with dominant frequency about 15 KHz. Typical receiver spacing is 6 inches, and

source-receiver near offset is 10 feet. The frequency shift method needs broad band signals and multiple receivers. Therefore, full waveform logs are suitable for the frequency shift method.

Waves in a fluid-filled borehole are very rich, including P-wave, S-wave, pseudo-Rayleigh wave, Stoneley wave, reverberant waves and so on. We use the short-time Fourier transform to estimate the centroid frequencies of these waves. A profile of centroid frequencies gives a new display of a full waveform log that shows the relative attenuation changes of these waves.

## WAVES IN A FLUID-FILLED BOREHOLE

The mathematical description of waves in a borehole is referred to, for example, White (1983) and Tsang & Rader (1979). There are two main types of waves in a fluid-filled borehole: body waves (P and S) and guided waves (pseudo-Rayleigh and Stoneley). In logging environment, body waves are critically refracted waves that travel vertically in the formation near the borehole wall with P-wave velocity or S-wave velocity. The S-wave, in fact, is a P-S-P conversion wave. When the S-wave velocity ($v_S$) of the formation is lower than the fluid velocity ($v_f$), the critically refracted S-wave will not exist in the borehole. The S-wave that incidents on the borehole wall at angles greater than the critical angle ($\beta_S$) undergoes a total reflection and propagates as a pseudo-Rayleigh wave with phase velocity $v_R$ ($v_f < v_R < v_S$). The pseudo-Rayleigh wave usually immediately follows the S wave. Since refraction into the formation at angles greater than $\beta_S$ is prohibited, there no energy leakage on each reflection. Therefore, the pseudo-Rayleigh wave exhibits relatively high amplitude. Its amplitude decays exponentially in the formation away from the borehole wall, but is oscillatory in the fluid. The dispersion of pseudo-Rayleigh is very large. Another guided wave is a pure surface wave with phase velocity lower than both $v_S$ and $v_f$, called as Stoneley wave. The amplitude of Stoneley wave decays exponentially in both the formation and the fluid away from the borehole wall. Its dispersion is mild.

## SHORT-TIME FOURIER TRANSFORM AND SPECTRAL CENTROID

A recorded seismogram trace contains different waves which arrive at different times. This means that the signal in the trace is time-variant. Time-frequency techniques, e.g., wavelet transform and short-time Fourier transform (STFT), are used for the time-

variant signal analysis which provides a representation of the data in a mixed time-frequency domain. Since STFT has direct physical meaning and is easier to be understood, we here use STFT to demonstrate our method. Wavelet transform is relatively new. In general, it is more suitable for time-frequency analysis (Ruskai, 1992).

Let $r(t)$ represent a seismic wave trace. The Fourier transform of $r(t)$ is defined as

$$R(f) = \int r(t)\exp(-i2\pi ft)dt \tag{1}$$

This *complete* Fourier transform represents the global (in time) characteristics of $r(t)$. It does not provide an adequate representation for each wave recorded in $r(t)$. If introducing a sliding window and computing the Fourier transform for the signal covered in this window for different window positions, we obtain the spectra of the signal $r(t)$ at different times. This is so-called short-time Fourier transform (e.g. Portnoff, 1980). The STFT for $r(t)$ is defined as

$$\hat{R}(\tau, f) = \int r(t)w(t-\tau)\exp(-i2\pi ft)dt, \tag{2}$$

where $w(t-\tau)$ is the sliding window and $\tau$ is the time where the STFT is performed. $\hat{R}(\tau, f)$ is a function of time and frequency which shows how the signal spectrum changes with time.

We often display seismograms as a gather — a profile of seismograms $r_i(t)$, where $r_i(t)$ is the $i^{th}$ trace in the gather. Performing STFT for seismograms $r_i(t)$, we get a three-variable function $\hat{R}_i(\tau, f)$. We can not show $\hat{R}_i(\tau, f)$ using a simple plot as the display for $r_i(t)$. In order to represent the major time-frequency property of $r_i(t)$ in a simple plot, we introduce the spectral centroid $f_i(\tau)$ defined as

$$f_i(\tau) = \frac{\int f|\hat{R}_i(\tau, f)|df}{\int |\hat{R}_i(\tau, f)|df}. \tag{3}$$

We can display $f_i(\tau)$ in a plot similar to that for $r_i(t)$. The centroid frequency $f_i(\tau)$ is like the instantaneous frequency of time signal $r_i(t)$.

## ATTENUATION ESTIMATION

Another motivation to introduce centroid frequency $f_i(\tau)$ is for seismic attenuation study, since $f_i(\tau)$ is directly related to attenuation coefficient (Quan & Harris, 1993). Assume that the seismic attenuation is linearly proportional to frequency. Then the attenuation response *H(f)* of the medium is determined by

$$H(f) = \exp(-f\alpha_o L), \tag{4}$$

where $L$ is the distance from a source to a receiver (note that we are discussing the logging problem), and $\alpha_o = \pi / (Qv)$ is attenuation coefficient. Here $Q$ is quality factor and $v$ is velocity. Let $S(f) = \exp[-(f - f_o)^2 / 2\sigma^2)]$ be the spectrum of an incident wave. Then the centroid frequency at the receiver is given as

$$f_R = \frac{\int fS(f)H(f)df}{\int S(f)H(f)df} = f_o - 2\sigma^2\alpha_o L,$$

or

$$f_o - f_R = 2\sigma^2\alpha_o L, \tag{5}$$

It can be seen from Eqn (5) that the frequency down shift $(f_o - f_R)$ is proportional to the attenuation coefficient $\alpha_o$. Therefore, a display of centroid frequencies $f_i(\tau)$ in Eqn (3) shows the relative changes in attenuation of different waves at different depths. We also need broad band signal so that the frequency shift is large enough for observation. The variance $\sigma^2$ of a typical sonic tool is about $10^8$ $(\text{Hz})^2$, which is suitable for frequency shift method. Since this method measures spectral centroid in stead of amplitude, it is relatively insensitive to geometric spreading and instrument gains.

The plot of centroid frequency $f_i(\tau)$ exhibits a similar pattern as amplitude display $r_i(t)$. That is, it still includes the information about wave travel time. Therefore, the plot of $f_i(\tau)$ can be used to correlate wave velocity and attenuation, and compare the relative attenuation of different waves.

Since the first arrival (P wave) is separable from other waves, it is possible to quantitatively measure P-wave attenuation using frequency shift method. Rewrite Eqn (5) as

$$\alpha_o = (f_{R_1} - f_{R_2}) / (2\sigma_{R_1}^2 L_{12}), \tag{6}$$

where $f_{R_1} - f_{R_2}$ is the centroid frequency difference between receivers 1 and 2, $L_{12}$ is the distance between receivers 1 and 2, and $\sigma_{R_1}^2$ is the variance of spectrum $\hat{R}_1(f)$ at receiver 1 (the one closer to the source) defined as

$$\sigma_{R_1}^2 = \frac{\int (f - f_{R_1})^2 |\hat{R}_1(f)| df}{\int |\hat{R}_1(f)| df}. \tag{7}$$

We choose a window that just covers the wavelet of the first arrival, and perform conventional Fourier transform to this signal being separated. Then using Eqns (6) and (7) we obtain the attenuation coefficient at each depth.

## SEMBLANCE CORRELATION

Semblance correlation is a common method of determining wave velocities from array full waveform data (e.g., Tittman, 1986). Here we also use this method to determine wave locations in a seismogram trace, since we need to identify where the waves are in a display of $f_i(\tau)$. Figure 1 shows 8 traces of an array recorded in Cajon Pass drillhole. Let $r_i(t)$ be the i$^{th}$ trace in an array record. The semblance of $n$ equally spaced receivers is defined as

$$S(\tau, \eta) = \frac{1}{n} \frac{\int [\sum_{i=1}^{n} r_i(t - (i-1)\eta\Delta l)]^2 w(t-\tau) dt}{\sum_{i=1}^{n} \int r_i^2(t - (i-1)\eta\Delta l) w(t-\tau) dt}, \tag{8}$$

where $\eta$ is slowness, $\Delta l$ is the receiver spacing, and $w(t-\tau)$ is a sliding window similar to that in STFT. We calculate all values of $\eta$ and $\tau$ having physically interesting meaning for Eqn (8). If a slowness value $\eta$ equals the slowness of a wave and the window just covers the same wavetrain, then $S(\tau,\eta)$ reaches a peak. Figure 2 is the semblance correlation of Figure 1, in which $S(\tau,\eta)$ are set to zeros for all $S(\tau,\eta) < 0.7$ to make the plot clear. It can

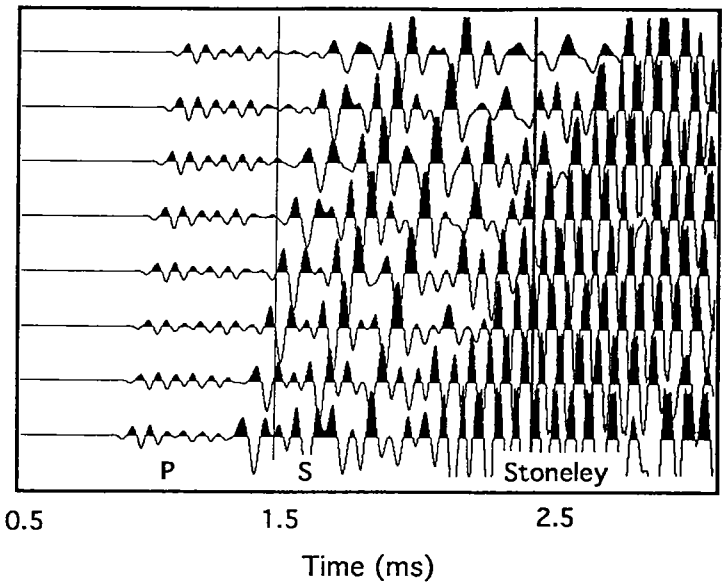


Figure 1. An array record (Depth =2540 ft) from Cajon full waveform log. reciever spacing is 6 in. Shot is 10 ft away from the first receiver.

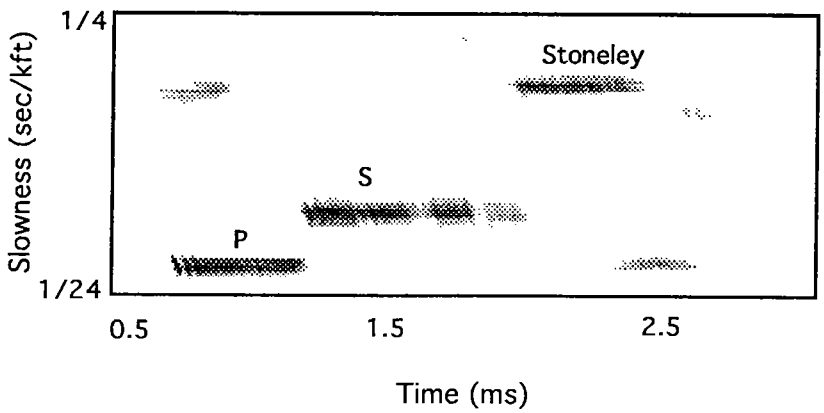


Figure 2. The semblance correlation of the record above. From this plot wave velocities and locations are determined.

kft/sec and Stoneley wave velocity $v_{st}$=4.8 kft/sec. Since the pseudo-Rayleigh wave immediately follows the S-wave, we can not separate them. Here and in the following we simply refer to the S wave together with the pseudo-Rayleigh wave as a S wave. With the semblance correlation in Figure 2 we identify wave types as shown in Figure 1. Note that the arrival time of P and S waves appearing in the data includes the travel time in borehole fluid. The calculated arrival time of P and S waves using the velocity obtained from the semblance are much smaller than the apparent arrival time in the log data, and therefore can not be directly used to identify the wave types in a seismogram trace.

## TESTS ON FIELD DATA

A full waveform sonic log recorded in Cajon Pass scientific drillhole is used for the test. The digital array sonic tool consists of 8 receivers with spacing of 6 inches and frequency band of 5-20 KHz. The first receiver is 10 feet away from the source. The time sampling interval is 0.01 ms. The log runs from 795 feet to 6008 feet. A section of 2540 – 2840 feet shown in Figure 3 is selected for the test. By performing short-time Fourier transform and calculating centroid frequencies (see Eqn (2) and (3)) for the data shown in Figure 3, we obtain a profile of centroid frequencies as shown in Figure 4.

Since the first arrival (P wave) is separable, let us estimate P-wave attenuation separately. A time window of 0.12 ms long is used to extract the first arrival, then zeros are padded to the signal in order to get a higher frequency resolution, Now the time length is 10.24 ms log, which corresponds to a sampling interval of 98 Hz in frequency domain. Figure 5 shows the velocity and center frequency logs of P wave. We align and stack the eight traces in an array, and compute a "center frequency log" shown in Figure 5(b). The velocity and center frequency curves correlate pretty well, but we can also find some interesting differences, such as those indicated by arrows. These differences may provide more information about rock properties than the velocity curve alone. The center frequency log may be interpreted as a P-wave attenuation log.

Theoretically, we can estimate the Q-value at each depth using the center frequencies recorded at successive receivers in an array (see Eqns (6) and (7)). In practice, however, we have two major problems: (1) the frequency responses of receivers in an array are not consistent; (2) the receiver spacing is too small (only 6 inches) so that the frequency change between two receivers is too small comparing with the noise and the non-consistency of the

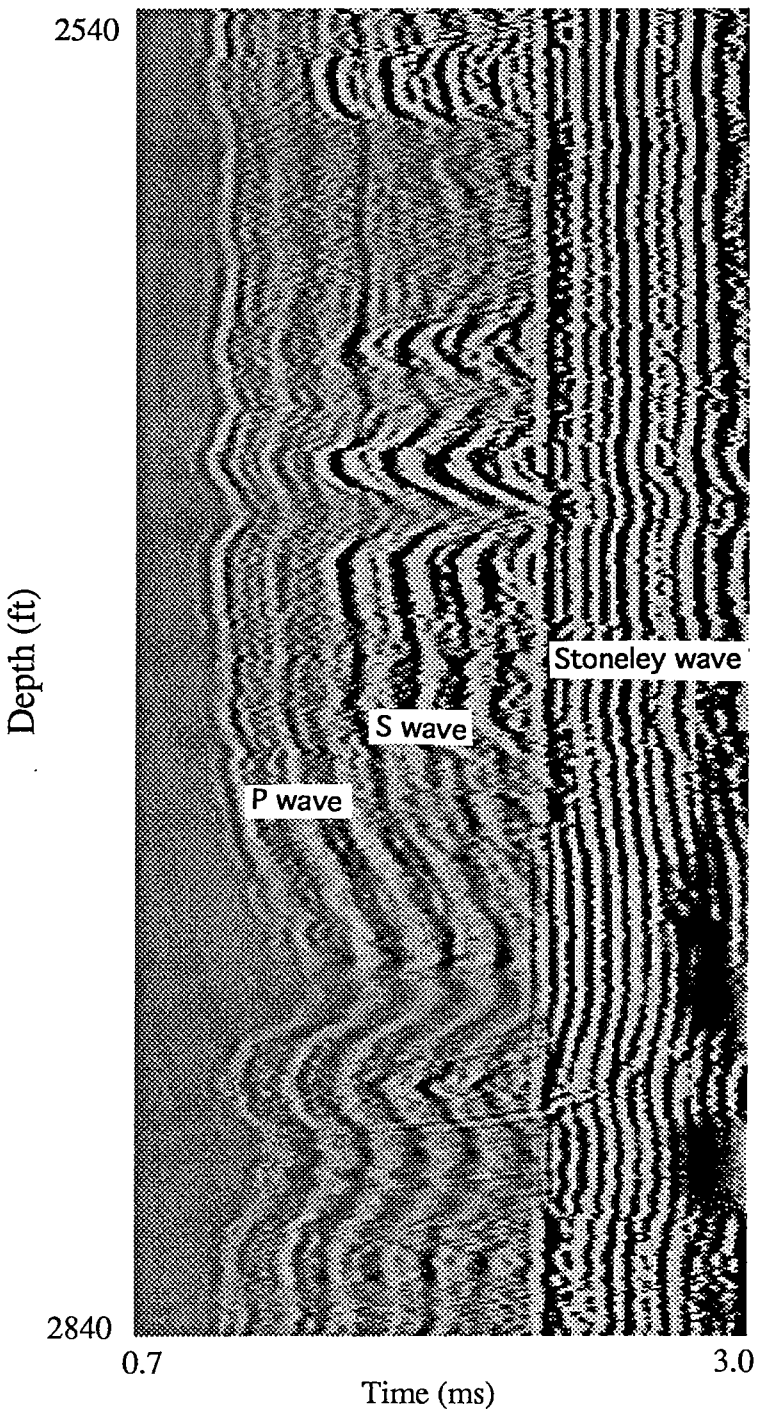


Figure 3. A portion of the Cajon full waveform log in the representation of amplitude. These are first traces in each arrary record.

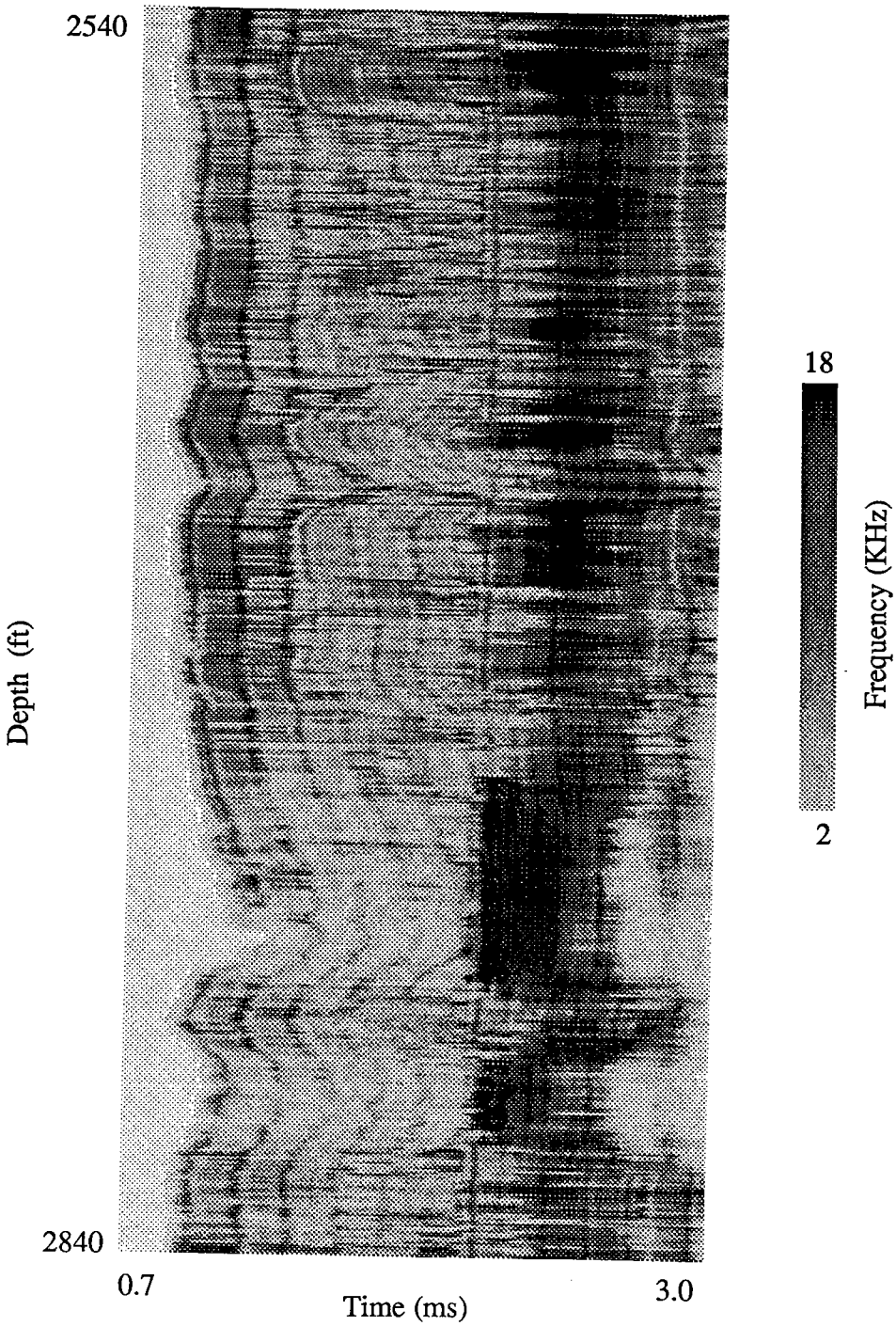


Figure 4. A centroid frequency representation of Cajon full waveform log. Short-time Fourier transform is used to obtain this time-dependent spectral centroid.

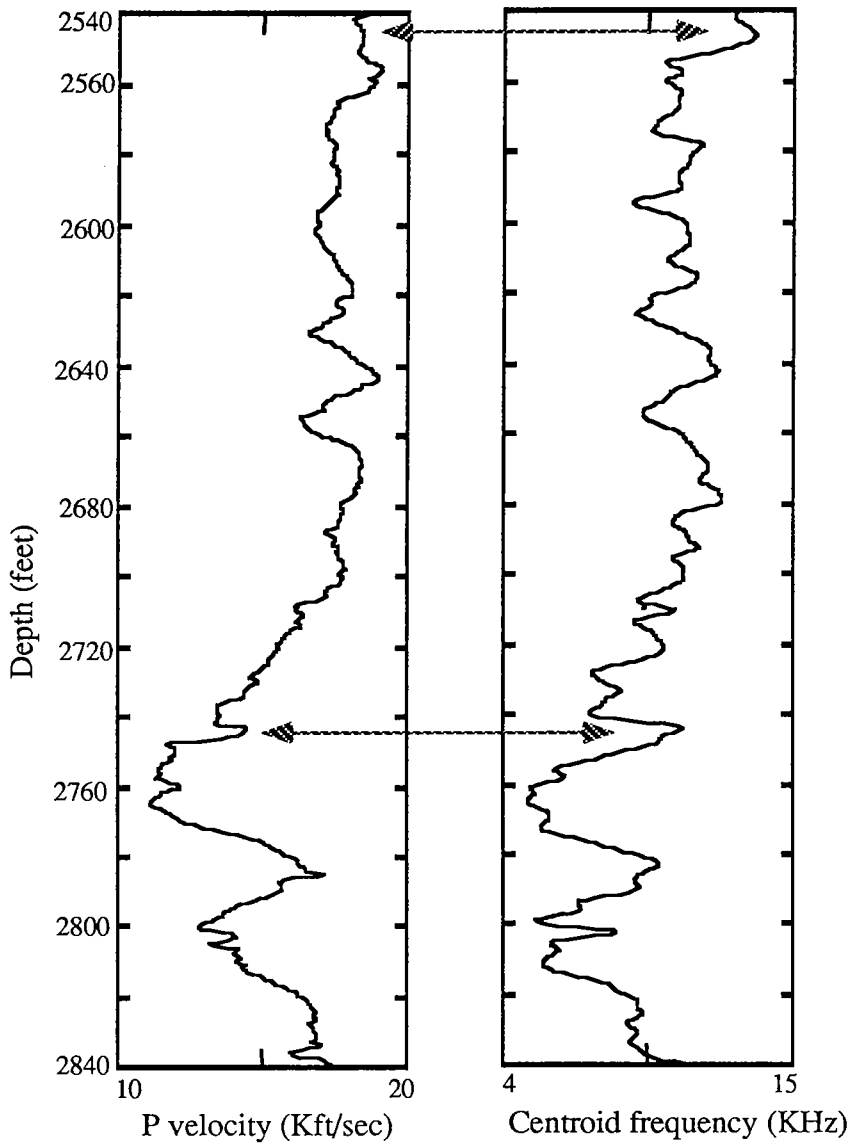


Figure 5. P wave velocity and centroid frequency. They have a good correlation except some depths, e.g. those shown by arrows.

receivers. Therefore, we need to calibrate the sonic tool and/or use a sonic tool with larger receiver spacing.

## CONCLUSIONS

The centroid frequency change is a direct indicator for seismic wave attenuation. For the full waveform sonic log, where high frequency and broad band signals are available, this indicator is sensitive. With the short-time Fourier transform we convert a full waveform log in amplitude to a log in centroid frequency that serves as a full wave attenuation log. By extracting first arrivals and calculating their centroid frequencies, we obtain a P-wave attenuation log. If we slightly modify the sonic tool and the logging procedure, making it more suitable for this method, we may quantitatively measure the P-wave attenuation for routine log interpretations.

## ACKNOWLEDGMENT

We would like to thank Daniel Moos for providing the log data.

## REFERENCES

Cheng, C., N. Toksöz & M. Willis, 1982, Determination of in situ attenuation from full waveform acoustic logs: JGR, **87**, No. B7, 4577-5484.

Dines, K. & A. Kak, 1979, Ultrasonic attenuation tomography of soft tissues: Ultrasonic Imaging, **1**, 16-33.

Engelhard, L, Th. Gross & F. Neupert, 1984, Comment on "Determination of in situ attenuation from full waveform acoustic logs": JGR, **89**, No. B5, 3400.

Fink, M., F. Hottier & J. Cardoso, 1983, Ultrasonic signal processing for in vivo attenuation measurement: Short time Fourier analysis: Ultrasonic Imaging, **5**, 117-135.

Portnoff, M., 1980, Time-frequency representation of digital signals and systems based on short-time Fourier analysis: IEEE Transaction on Acoustics, Speech, and Signal Processing, **ASSP-28**, No. 1,

Quan, Y & J. Harris, 1993, Seismic attenuation tomography based on centroid frequency shift: STP Report, **4**, No. 1, (this volume).

Ruskai, M. Ed, 1992, Wavelets and their applications: Jones and Bartlett Publishers
Tittman, J., 1986, Geophysical well logging: Academic Press.

Tsang, L., & D. Rader, 1979, Numerical evaluation of the transient acoustic waveform due to a point source in a fluid-filled borehole: Geophysics, **44**, 1706-1720.

White, J., 1983, Underground sound: Elsevier.